ESTIMATION OF ELONGATIONAL VISCOSITY OF POLYMERS FOR ACCURATE PREDICTION OF JUNCTURE LOSSES IN INJECTION MOLDING

Mahesh Gupta
Mechanical Engineering-Engineering Mechanics Department
Michigan Technological University
Houghton, MI 49931

Abstract

A new elongational viscosity model along with the Carreau-Yasuda model for shear viscosity is used for a finite element simulation of the flow in a capillary rheometer. The entrance pressure loss predicted by the finite element flow simulation is matched with the corresponding experimental data to predict the parameters in the new elongational viscosity model.

Introduction

Since the thickness of most plastic parts is small, typically the flow during the filling stage of injection molding is highly shear dominated. Therefore, the generalized Newtonian constitutive models with shear thinning viscosity have been successfully employed to accurately simulate the mold filling process [1]. However, in certain regions of the mold, such as the runners, gates and portions of mold cavity with abrupt changes in thickness, polymer melt goes through a significant elongational deformation. The pressure gradient in these regions with elongation-dominated flow, predicted by a generalized Newtonian formulation can be significantly smaller than the pressure gradient encountered in the molding process [2]. The primary reason for the poor prediction of elongation-dominated flow, is the low elongational viscosity of the generalized Newtonian models [3]. The long chain polymer molecules exhibit stiff resistance to an elongational deformation. Therefore, the elongational viscosity of a polymer, which is defined as the ratio of the elongational stress to elongational strain rate, is very high. An accurate knowledge of the elongational viscosity of a polymer is important for simulating the elongation-dominated flows.

Various techniques such as uniaxial extension, lubricated compression, fiber spinning, bubble collapse, stagnation flow, etc., have been used in the past to experimentally characterize the elongational viscosity of polymers. A good review of these techniques and the difficulties associated with each of these techniques is presented by Macosko in reference [4]. Among these, the most commonly used technique is the uniaxial extension. An elongational rheometer using uniaxial extension, which is based upon Meissner's work [5], is currently marketed by Rheometric Scientific, Inc. [6]. However, maintaining a steady uniaxial extensional deformation is difficult at a high elongation rate [4]. Therefore, Meissner's technique can be used to determine elongational viscosity only at very low elongation rates ($< 10\ s^{-1}$). Also, Meissner's technique can only be used for highly viscous melts. Since the deformation rate in injection molding can range from 1,000 to 100,000 1/s, this technique cannot provide the elongational viscosity data required for injection molding simulation.

Due to the difficulties associated with direct measurement of elongational viscosity of a polymer, the flow in a channel with abrupt contraction (entrance flow) has often been used for an indirect measurement of elongational viscosity [4]. Since a polymer going through an abrupt contraction experiences a large elongational deformation, a steep pressure drop, called entrance pressure loss, is encountered near the abrupt contraction. The value to entrance pressure loss, which depends upon the flow rate in the channel, can be used for an indirect measurement of the strain-rate dependence of the elongational viscosity of a polymer. The advantage of the entrance flow method for measuring elongational viscosity is its applicability at high elongation rate. Furthermore, an existing capillary rheometer, which is commonly used for measuring shear viscosity, can also be used for elongational viscosity estimation.

Assuming that the pressure loss in an entrance flow can be obtained by summing the pressure drops due to shear and elongational deformations, Cogswell [7] obtained separate expressions for these two pressure drops. To further simplify the analysis, Cogswell made several other assumptions listed below:

1. shear stress and shear rate are related by power-law model
2. elongational viscosity is constant
3. the interface between the recirculation region and the main flow is a straight line (funnel-shaped flow)
4. no-slip on the interface between recirculation region and the main flow
5. fully developed flow with zero radial velocity
6. neglect Weissenberg-Robinowich correction [3]
7. inertia-less, incompressible flow with no normal stresses in shear.

With these assumptions, Cogswell performed a force balance on a differential section of the funnel-shaped entry region near abrupt contraction. By integrating the

expressions thus obtained, Cogswell obtained the following expressions for average elongation rate in entrance flow (Eqn. (1)) and the corresponding elongational viscosity (Eqn. (2)) for an axisymmetric flow.

$$\dot{\varepsilon} = \frac{4\tau_w \dot{\gamma}_a}{3(n+1)\Delta p_e} \tag{1}$$

$$\eta_e = \frac{3(n+1)\Delta p_e}{8\dot{\varepsilon}} \tag{2}$$

where $\tau_w = \Delta pR/2L$ is the shear stress at the capillary wall, $\dot{\gamma}_a = 4Q/(\pi R^3)$, Δp_e is the entrance pressure loss, Δp is the pressure drop in the capillary, R and L are the radius and length of the capillary, respectively, and $\dot{\varepsilon}$ is the elongation rate.

By removing some of the assumptions in the Cogswell's analysis, Binding [8] obtained a more accurate expression for entrance pressure loss in an abrupt contraction. However, many of the assumptions in Cogswell's analysis, listed below, are retained in Binding's analysis:

1. power-law model for shear viscosity ($\eta_s = A\dot{\gamma}^{n-1}$) as well as for elongational viscosity ($\eta_e = B\dot{\varepsilon}^{m-1}$)
2. the interface between the recirculation region and the main flow is a straight line (funnel-shaped flow)
3. no-slip on the interface between recirculation region and the main flow
4. fully developed flow with no radial velocity
5. $|dR/dz| \ll 1$, such that the terms involving $(dR/dz)^2$ and d^2R/dz^2 can be neglected, implying a large recirculation zone
6. energy consumed in recirculation zone can be neglected
7. inertia-loss, incompressible flow with no normal stresses in shear.

With these simplifications, Binding employed energy principles to obtain the following equation for entrance pressure loss:

$$\Delta p_e = \frac{2A(1+m)^2}{3m^2(1+n)^2}\left[\frac{mB(3n+1)n^m I_{nm}}{A}\right]^{\frac{1}{m+1}} \times \dot{\gamma}_w^{\frac{m(n+1)}{m+1}} \left[1-\alpha^{\frac{3m(n+1)}{m+1}}\right] \tag{3}$$

where $\alpha = R_0/R_1$, with R_0 and R_1 being the radii of downstream and upstream channels respectively, $I_{nm} = \int_0^1 \left|(3n+1)\rho^{1+1/n}/n - 2\right|^{m+1} \rho d\rho$, and the shear rate at capillary wall $\dot{\gamma}_w = (3n+1)Q/(\pi n R_0^3)$. If the power-law model for shear viscosity of a polymer, and entrance pressure loss is known for two different flow rates in an abrupt contraction, Eqn. (3) can be used to determine the power-law model (B, m) for the elongational viscosity of a polymer.

By using independent power-law models for shear and elongational viscosities, Gupta [9] analyzed the effect of elongational viscosity on vortex formation and entrance pressure loss in an axisymmetric 4:1 entrance flow. Similar analysis of the flow in a channel with abrupt contraction for the planar and the three-dimensional cases were later presented in references [10] and [11], respectively. In references, [9 - 11], the truncated power-law model was used for the shear viscosity as well as for the elongational viscosity in the axisymmetric and planar cases. This approach of simulating polymeric flows is not only frame invariant, but predicted velocity and pressure distributions for a general 3-D flow are also identical to those from the generalized Newtonian formulation, if the specified shear and elongational viscosity models are such that $\eta_e(e_{II}) = 3\eta_s(e_{II})$ for axisymmetric flows and $\eta_e(e_{II}) = 4\eta_s(e_{II})$ for planar flows, with e_{II} being the second invariant of the strain rate tensor. More recently, using the same approach, Sarkar and Gupta [12] employed the Carreau model for shear viscosity and a modification of Carreau model for elongational viscosity.

$$\eta_s = \eta_0\left(1+(\lambda e_{II})^2\right)^{\frac{n-1}{2}} \tag{4}$$

$$\eta_e = \eta_0\left[3+\delta\left\{1-\frac{1}{\sqrt{1+(\lambda_1 e_{II})^2}}\right\}\right]\left[1+(\lambda_2 e_{II})^2\right]^{\frac{m-1}{2}} \tag{5}$$

The elongational viscosity model in Eqn. (5), reduces to the Carreau model for $\delta = 0$ with the elongational viscosity parameters λ_2 and m replacing λ and n respectively, in the shear viscosity model. The two additional parameters λ_1 and δ in Eqn. (5), control the increase in the elongational viscosity in the elongation-thickening region [12].

In the present work, we have used the Carreau model for shear viscosity (Eqn. (4)) and model proposed by Sarkar and Gupta for elongational viscosity (Eqn. (5)). Knowing the shear and elongational viscosity parameters, a finite element simulation of the entrance flow is performed. The finite element simulation of the entrance flow eliminates most of the simplifying assumptions of Cogswell and Binding's analysis. However, the flow simulation still assumes an inertia-less, incompressible flow with no normal stresses in a shear flow. With a knowledge of the shear viscosity and entrance pressure loss, using the procedure presented in the next section, the elongational viscosity parameter are optimized such that the difference between the experimental values of entrance pressure loss and the corresponding predictions from the finite element simulation is minimized.

Estimation Procedure for Elongational Viscosity Parameters

In our earlier publication [13], we reported a global minimization procedure to optimize the elongational viscosity parameters. In particular, starting with an initial guess for the four parameters, the simplex optimization scheme [13] was used to iteratively improve their values such that the difference between experimental and predicted values of entrance loss is minimized. Even though such a global minimization procedure is more rigorous, and attempts to minimize the error over the complete range of flow rate vs entrance loss data, it requires very large amount of computational time, and convergence to the optimal values is prohibitively slow at times.

To improve the efficiency of the estimation software, in the present work, only the values of λ_2 and *m* are optimized simultaneously, which is followed by individual optimization of δ and λ_1. It should be noted that parameters λ_2 and *m* affect the elongational viscosity only in the power-law region at high strain rate, whereas δ and λ_1 control the shape of the elongational-thickening portion of the viscosity curve [12]. In particular, λ_1 determines the strain rate for onset of elongation thickening region, whereas δ controls the total increase in the viscosity in the thickening region. Since δ and λ_1, and λ_2 and *m* affect the elongational viscosity in different regions, values of δ and λ_1, and those of λ_2 and *m* can be optimized independently. Because of this localized effects of δ and λ_1, and that of λ_2 and *m*, if all the entrance pressure loss data is in power-law region, optimization of the elongation-thickening parameters is difficult and vice versa. The localized effects of power-law (λ_2 and *m*) and elongation-thickening (δ and λ_1) parameters on elongation viscosity curve, result in the inefficiency of the global minimization scheme.

To optimize the four elongational viscosity parameters, the experimental data for entrance loss is required for at least four different flow rates. Two of these points should be in the power-law region (to determine λ_2 and *m*). If the polymer melt exhibits the elongation-thickening region, one of the points should be in the elongation-thickening region (to determine δ) and the fourth point should be in the transition region between Newtonian and elongation thickening behavior (to determine λ_1). Typically, entrance pressure loss vs flow rate data is available at a large number of points (» 4). Since an entrance flow simulation for a fixed set of elongational viscosity parameters requires significant amount of computation time (from 2 - 20 minutes on a Sun workstation, depending upon the number of nodes in the finite element mesh and number of iterations required for convergence), and the entrance flow is repeatedly simulated at the entrance loss vs flow rate data points, a very large computation time is required for estimation of elongational viscosity parameters, if all the data points are used in the optimization scheme. Therefore, a systematic scheme, described in the next paragraph, is employed in the present work to select the four entrance loss vs flow rate data points for estimation of the four elongational viscosity parameters.

Estimation procedure of elongational viscosity parameters starts with an initial guess for the four parameters. The software allows the user to specify an initial estimate of the four parameters. Otherwise, the software automatically initializes the elongational viscosity parameters based upon the generalized Newtonian formulation, that is $\eta_e(e_{II}) = 3\eta_s(e_{II})$, or from the values obtained by Binding's analysis. It should be noted that in both of these cases $\delta = 0$, and λ_1 have no affect on elongational viscosity if $\delta = 0$. Therefore, only λ_2 and *m* are initialized. Since the experimental data at higher flow rate is expected to be in the power-law region, the data point at the highest flow rate and another data point with flow rate of about one-hundredth of the highest flow rate are used for estimation of power-law parameters λ_2 and *m*. Once the two points for estimation of power-law parameters are identified, as shown in Fig. 1, the optimal values of λ_2 and *m* are determined by alternating the Newton-Raphson method for λ_2 and *m*. The function f_m and f_{λ_2} are the differences in experimental and predicted values of entrance pressure loss for points with the highest flow rate and one-hundredth of the highest flow rate, respectively. At this point of the algorithm λ_2 and *m* have been identified, however δ is zero and λ_1 is also unknown. With $\delta = 0$ and using the estimated value of λ_2 and *m* in the elongational viscosity curve, the data point having the largest difference between experimental and predicted value of entrance loss is used for optimization of δ. If some of the points in the entrance loss vs flow rate data are in the Newtonian range of elongational viscosity, experimental value of entrance loss for these points should match with the predicted entrance loss for $\delta = 0$ in the elongational viscosity model (Eqn. (5)). Therefore, starting with the lowest flow rate, the first experimental point with greater than 10% error between experimental and predicted entrance loss is used to optimize the value of λ_1. Before starting the optimization of δ, the parameter λ_1 is initialized to a very large value $\lambda_2 = \lambda_1 \times 10^{10}$, which implies that elongation thickening is assumed to start at a very low elongation rate. Using the point identified above for optimization of δ, as shown in Fig. 1, Newton-Raphson method is used again to estimate the value δ. The function f_δ in Fig. 1 is the difference between experimental and predicted entrance loss for the point being used for optimization of δ. Finally, the parameter λ_1 is estimated by minimizing the entrance loss

error for the point identified above for λ_1 optimization. The bracketing and bisection method [14] is used for optimizing the value of λ_1.

Experimental Data

A Goettlfert Rheometer 1000 was used to measure the viscosity and entrance pressure loss. The diameter of capillary in all the dies used was 1 mm. The pressure loss vs capillary length curves for dies with capillary length of 5, 20, 30 and 40 mm were extrapolated to obtain the entrance pressure loss. The Weissenberg-Robinowitch correction was applied to account for the non-parabolic velocity profile. A Bohlin VOR with 25 mm parallel plates was used to measure the shear viscosity at low shear rates. in the experiments, a low density polyethylene (Dow 132i) was used. The entrance pressure loss and shear viscosity was measured for two different temperatures - 160 and 175 ^{o}C.

Results and Discussion

In this paper, the elongational viscosity for a low density polyethylene (Dow 132i) is estimated at two different temperatures. For Dow 132i at 160 and 175 ^{o}C, the experimental data for entrance pressure loss at various flow rates is shown in Fig. 2. As expected, the entrance loss increases significantly as the flow rate is increased. At a fixed flow rate the entrance loss is higher for the lower temperature. The shear viscosity for Dow 132i, which is obtained by fitting the Carreau model to the experimental data, is shown in Fig. 3. The Carreau model parameters for the shear viscosity of Dow 132i are as follows:

160^{o}C: $\eta_0 = 2.6\times 10^5$ Pa.s $\quad \lambda = 37.35\ s^{-1}$ $\quad n = 0.3409$

175^{o}C: $\eta_0 = 2.1\times 10^5$ Pa.s $\quad \lambda = 31.69\ s^{-1}$ $\quad n = 0.3409$

The entrance loss data in Fig. 2 and the Carreau model for shear viscosity in Fig. 3, was used in the present work to predict the elongational viscosity employing the algorithm discussed earlier in this paper. For the two different temperatures, the predicted elongational viscosity is shown in Fig. 3. It should be noted that the predicted elongational viscosity in Fig. 3 is plotted against $e_{II} = \sqrt{3}\dot{\varepsilon}$. The power-law parameters for the elongational viscosity were predicted using the entrance pressure loss value for flow rates of 5.65 and 339 mm^3/s for 160^{o}C and for 5.66 and 452 mm^3/s for 175^{o}C. With these control points the elongational viscosity parameters are as follows:

160^{o}C: $\lambda_2 = 1.61\ s^{-1}$ $\quad m = 0.281$

175^{o}C: $\lambda_2 = 2.35\ s^{-1}$ $\quad m = 0.317$

With these values of power-law parameters for elongational viscosity, the largest difference in the experimental and predicted entrance pressure loss is at the lowest flow rates - 1.13 and 0.565 mm^3/s for 160 and 175^{o}C, respectively. For each of the two temperatures, optimization of the elongational viscosity parameter δ was attempted by using the entrance loss data at these two points. However, at both the temperatures, the predicted entrance loss at the lowest flow rates in Fig. 2, was found to be highly insensitive to a change in δ, indicating that even the two points at the lowest flow rates in Fig. 2 are in the elongation-thinning region of elongational viscosity. Therefore, for Dow 132i the elongational-thickening parameters (δ, λ_1) in Eqn. (5) could not be predicted using the available entrance loss data. Accordingly, the elongational viscosity curves for Dow 132i in Fig. 3 do not show any elongation-thickening behavior. However, the elongational viscosity for Dow 132i may have an elongation-thickening region for $e_{II} < 1\ s^{-1}$, which can only be captured using our algorithm if the entrance loss data is available at smaller flow rates. Since the entrance loss at lower flow rates may be too small to measure with a reasonable accuracy, elongational viscosity at lower elongation rates may not be predicted accurately using the current technique. This is not a serious limitation of this technique because the elongation rates in polymer processing are typically quite high. Also, if the elongational viscosity at lower elongation rates can be measured by other experimental techniques mentioned earlier in the paper, a composite elongational-viscosity may be constructed by finding the elongation-thickening parameters (δ, λ_1) using the elongational viscosity measured by direct experimental techniques and the power-law parameters (λ_2, m) from the entrance pressure loss measurement.

For Dow 132i, the elongational viscosities at 160 and 175^{o}C, predicted by Cogswell's and Binding's analysis are also shown in Fig. 3. Interestingly, even though Cogswell's and Binding's predictions are based upon numerous simplifying assumptions, the elongational viscosity predicted by the two analyses are in good agreement with the predictions from the present work.

Acknowledgement

The author would like to thank Prof. F. A. Morrison for making the experimental data for entrance pressure loss and shear viscosity available to us.

References

1. H. H. Chiang, C. A. Hieber and K. K. Wang, *Polym. Eng. Sci.*, **31**, 116 (1991).
2. P. Brincat, C. Friedl and K. Talwar, *SPE ANTEC Technical Papers*, **44**, 552 (1998).
3. R. B. Bird, R. C. Armstrong and O. Hassager, *Dynamics of Polymeric Liquids*, Vol. 1 and 2, John Wiley, New York (1987).
4. C. W. Macosko, *Rheology Principles, Measurements and Applications*, VCH, New York (1994).

5. J. Meissner, *Rheol. Acta*., **8**, 78 (1969).
6. Rheometrics Scientific, Inc. One Possumtown Road, Piscataway, NJ 08854, USA (http://www.rheosci.com).
7. F. N. Cogswell, *Polym. Eng. Sci.*, **12**, 64 (1972).
8. D. M. Binding, *J. Non-Newtonian Fluid Mech.*, **27**, 193 (1988).
9. M. Gupta, *Polym. Eng. Sci.*, **40**, 23 (2000).
10. M. Gupta, "Simulation of Planar Entrance Flow Using Strain-Rate-Dependent Shear and Elongational Viscosities", *J. Reinforced Plastics and Composites*, (In press).
11. M. Gupta, *SPE ANTEC Tech. Papers*, **45**, 83 (1999).
12. D. Sarkar and M. Gupta., "An Investigation of the Effect of Elongational Viscosity on Entrance Flow", to be presented at ASME-IMECE, November 2000.
13. D. Sarkar and M. Gupta, "Estimation of Elongational Viscosity using Entrance Flow Simulation", to be presented at ASME-IMECE, November 2000.
14. W. H. Press, B. P. Flanery, S. A. Teukolsky and W. T. Vetterling, Numerical Recipes, Cambridge University Press, Cambridge (1989).

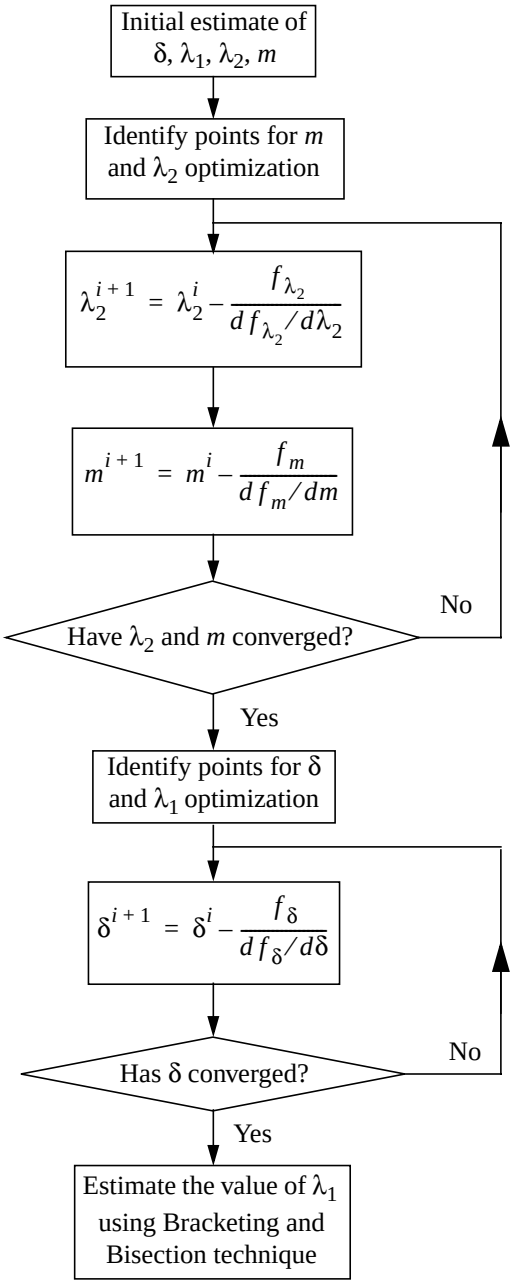

Fig. 1. Flow chart for optimization of elongational viscosity parameters.

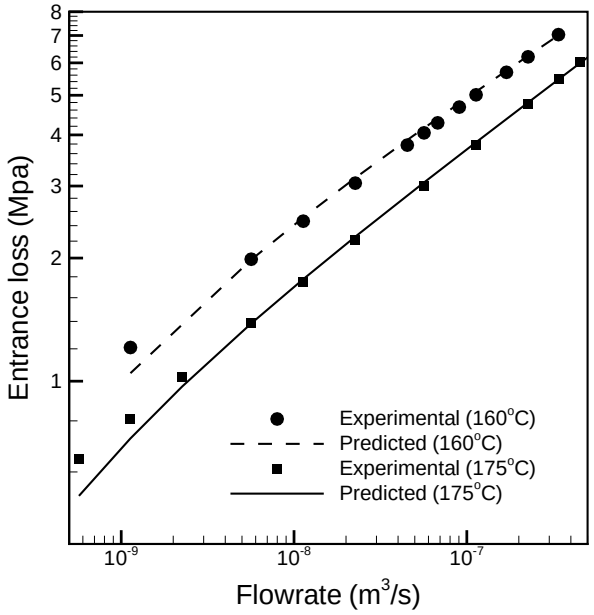

Fig. 2. Entrance loss vs. Flow rate for Dow 132i.

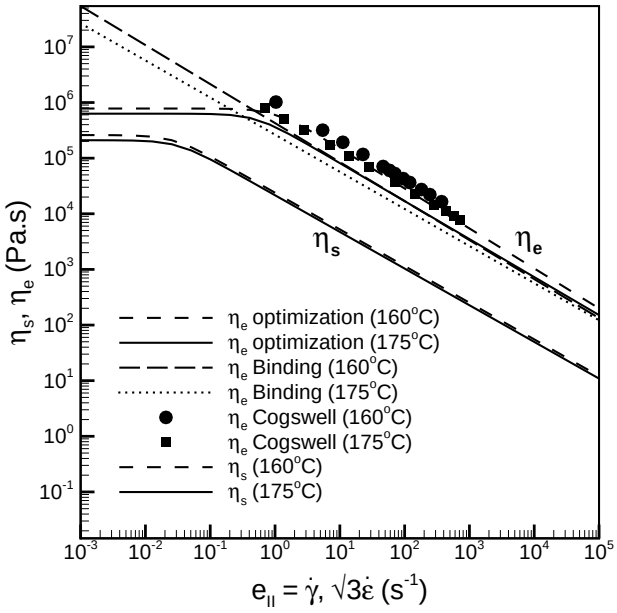

Fig. 3. Variation of shear (η_s) and elongational (η_e) viscosities of Dow132i with the second invariant of strain-rate tensor (e_{II}).